

PROGRAM OF TELLURIC LINES MONITORING

I. Vince¹, P. Kos², O. Latković¹, N. Martinović³, M. Gošić³ and J. Stojadinović³

¹*Astronomical Observatory, Volgina 7, 11160 Belgrade 74, Serbia*

²*University Paris 7 - Denis Diderot, France*

³*Department of Astronomy, Faculty of Mathematics, Studentski trg 16, 11000 Belgrade, Serbia*

(Received: October 5, 2006; Accepted: October 26, 2006)

SUMMARY: A new observational program of telluric lines monitoring was introduced at Belgrade Astronomical Observatory. The ultimate goal of this program is to investigate the properties of Earth's atmosphere through modeling the observed profiles of telluric lines. The program is intended to observe infrared molecular oxygen lines that were selected according to spectral sensitivity of the available CCD camera. In this paper we give the initial and the final selection criteria for spectral lines included in the program, the description of equipment and procedures used for observations and reduction, a review of preliminary observational results with the estimated precision, and a short discussion on the comparison of the theoretical predictions and the measurements.

Key words. Techniques: spectroscopic – Line: profiles – Instrumentation: spectrographs

1. INTRODUCTION

In the framework of collaboration between Solar-Terrestrial Influence Laboratory at Stara Zagora, Bulgaria, and Belgrade Astronomical Observatory, the establishment of a long-term observational program for monitoring telluric spectral lines, to be carried out using the solar spectrograph of the Belgrade Astronomical Observatory (Kubicela 1975), was planned. The program is intended to obtain information about the Earth's atmosphere through modeling the observed profiles of telluric lines (Guineva and Werner 2006).

The solar spectrograph at the Belgrade Astronomical Observatory was adapted for this purpose, and in summer 2006 a preliminary set of 13 molecular oxygen spectral lines with odd rotational quantum numbers from 1 to 25 of P branch from B atmospheric band was observed. These observations were used to adjust our spectrograph for observation

in the infrared spectral region, to estimate the precision of measurements and to make a final selection of most suitable lines.

The precision of our measurements was evaluated by fitting the observed equivalent widths of selected telluric lines with theoretical predictions. For the six lines with rotational quantum numbers from 9 to 19 the agreement between observations and theory is excellent. For the rest of the lines the agreement is also good, but as will be shown later, we decided to discard them from the selection.

2. THE OBSERVATIONAL PROGRAM

According to the goals of the aforementioned collaboration, a program aimed at monitoring and studying the changes of a number of telluric line profiles is established at the solar spectrograph of Belgrade Astronomical Observatory. In this section we

describe in detail the process of selection of the spectral lines, the arrangement of the solar spectrograph and the methods of image reduction.

2.1. Selection of spectral lines

Preliminary inspection of telluric lines in a solar spectral atlas (Beckers *et al.* 1976) showed that the following lines should be suitable for this study: rotational-electronic absorption lines of molecular oxygen in (0,0) A and (1,0) B atmospheric bands of the infrared region of Fraunhofer spectrum. Spectral sensitivity of our CCD detector and the effectiveness of spectrograph optics further limit the observable spectral range to the (1,0) B band region located approximately between about 687 nm and 697 nm. Within this region the choice of spectral lines to be observed was governed by the following criteria:

- The spectral line should be strong enough for precise measurement of line profile,
- If possible, the spectral line should have a blend-free line profile
- A well-defined continuum should be present in the vicinity of the line,
- The selected lines should have well established molecular parameters,
- Spectral lines should belong to a known rotational branch, since then their relative intensities can be determined from theoretical considerations.

According to these requirements we have chosen 13 spectral lines of molecular oxygen (with nuclei of the major oxygen isotope) from the P branch of the (1,0) B spectral band, with odd rotational quantum numbers from $J=1$ to $J=25$. Even values of the rotational quantum numbers are not allowed in the ground electronic and vibrational states. Each line with a given odd rotational quantum number is split with spacing of about 0.09 nm (see Fig. 1). This splitting is due to weak coupling of spin and magnetic angular momentum. The doubled is described with a single rotational quantum number. Thus, every selected line has two relatively strong components, with the exception of the line with $J=1$, which has only one component.

Although these lines belong to a spin-forbidden transition, large abundance of molecular oxygen in the Earth's atmosphere and the long atmospheric path-length of solar light give rise to strong spectral lines very suitable for measurements.

The selected spectral lines are listed in Table 1. They are located in spectral region from 688 nm to 694 nm. The columns of Table 1 contain respectively: the rotational quantum number of the lower energy level of transition, the wavelength of the first and the second component of the doublet and the corresponding wavelengths in the next overlapping higher order spectrum in visual region (see later for explanation).

Table 1. The list of selected spectral lines and the corresponding visual wavelengths.

J	λ_I [nm]	λ_{II} [nm]	λ_{IV} [nm]	λ_{IIV} [nm]
1	688.3833	-	516.2875	-
3	688.5754	688.6743	516.4316	516.5057
5	688.8948	688.9903	516.6711	516.7427
7	689.2369	689.3309	516.9277	516.9982
9	689.6037	689.6965	517.2028	517.2724
11	689.9954	690.0868	517.4966	517.5651
13	690.4117	690.5023	517.8088	517.8767
15	690.8534	690.9431	518.1401	518.2073
17	691.3200	691.409	518.49	518.5568
19	691.8122	691.9002	518.8592	518.9252
21	692.3369	692.4164	519.2527	519.3123
23	692.8728	692.9599	519.6546	519.7199
25	693.4422	693.528	520.0817	520.146

To estimate the systematic errors in our measurements (for example, instrumental errors or errors due to blending of line profiles, errors of measurements) we used a simplified theory of molecular spectral line formation (see for example Schadee 1964, 1966). The following relation between the observed equivalent widths (EW_J) in one vibrational electronic band and the rotational quantum number (J) exists:

$$\ln \left(\frac{EW_J}{S_J} \right) = C_1 + C_2 \cdot \frac{B}{T} \cdot J(J+1),$$

where S_J is the rotational line strength, C_1 is a constant that is related to the number of absorbing molecule, B is the rotational constant of the lower energy level of transition (it is constant for all lines in a given band), T is the absolute temperature, and

$$C_2 = \frac{h \cdot c}{k},$$

where h and k are the Planck and the Boltzmann constants, respectively, and c is the velocity of light. The rotational line strength S_J is proportional to the statistical weight ($2J+1$) of the rotational level:

$$S_J = C_3(2J+1).$$

The constant C_3 depends on the type of electronic transition. By combining these equations, the following expression results:

$$\ln \left(\frac{EW_J}{2J+1} \right) = C_4 + C_2 \cdot \frac{B}{T} \cdot J(J+1),$$

where C_4 is a new constant derived from C_1 and C_3 .

If we assume that the temperature of atmosphere is constant during one set of observation, this equation can be further simplified:

$$\ln\left(\frac{EW_J}{2J+1}\right) = C_4 + C_5 \cdot J(J+1).$$

The relation between EW_J and $J(J+1)$ is linear. Therefore, the deviation of observed points from linear fit through these points can help us recognize systematic errors in measurements of a particular spectral line, allowing to choose which spectral lines in one electronic band are suitable for further investigation.

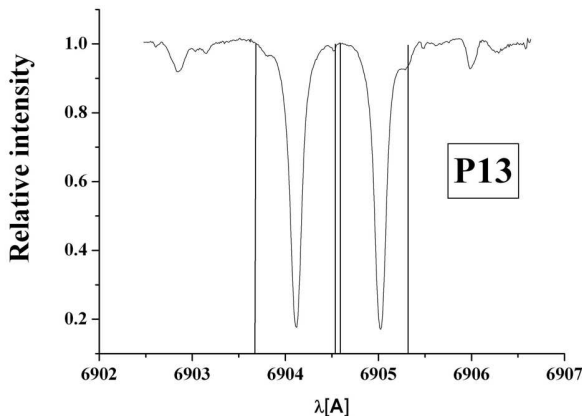


Fig. 1. The two components of the spectral line with rotational quantum number $J=13$ (observation was performed on July 14, 2006 at Belgrade Astronomical Observatory).

2.2. Observations and reduction

Spectroscopic observations of selected telluric lines were performed at the solar telescope of Belgrade Astronomical Observatory. The solar telescope is equipped with a Litrow type spectrograph (Litrow achromatic objective (diameter 20cm) with effective focal length of 900 cm) with 154x206 mm size Bausch and Lomb replica grating of 600 1/mm, and blazed angle in green spectral region in 5th spectral order. Running of another observational program ("Sun as a star", see e.g. Vince et al. 1988) required the spectrograph to be fed by sunlight without imaging optics, directly through the entrance slit which forms a pinhole image of the Sun on the optical grating. The observations were made in third spectral order where the blazing is in infrared range of spectrum. A slit width of 75 μm was used, that produced about 8 cm coherent light at grating in pinhole imaging mode, achieving a spectral resolution of about 10^5 in third spectral order. The 9 m effective focal length of camera lens allows linear dispersion in focal plane of 20.8 mm/nm (about 900 pixels/nm) at $\lambda \approx 690$ nm in third spectral order.

The detector is a SBIG ST6 CCD camera. The CCD camera's chip total array area is 8.6x6.5

mm (375x242 pixel array) with pixel size of 23x27 μm , and the sensitivity of the camera covers the spectral region from about 400 nm to 900 nm with the higher responsivity of about 50%-70% at 680 nm. As the chip covers only about 0.4 nm of third order spectrum in focal plane of our spectrograph, only one doublet can be observed at a time (see Fig. 2). Consequently, every observational set consists of 13 CCD spectrograms centered at wavelengths as indicated in the second and third columns of Table 1.

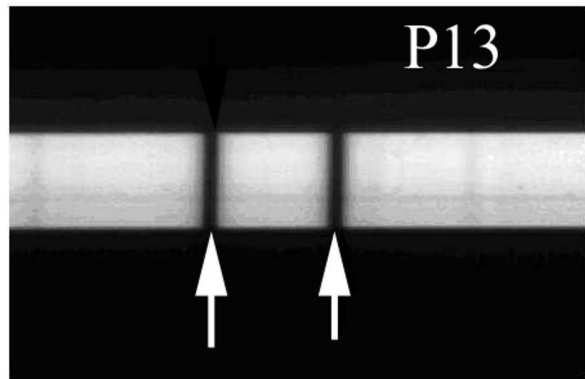


Fig. 2. The CCD image of the solar spectrum with the doublet of P13.

The readout electronics of our CCD camera uses a 16 bit A/D converter, which converts the signal into a digital number (count) from 0 to 65535. During the observation, the exposure duration was adjusted to achieve the count values from 30000 to 40000 in continuum in order to avoid the pixel saturation at higher counts (at about 45000-50000). This allows very accurate signal measurements, which are, of course, degraded by various noises. Noise in observed spectra comes from photon noise, seeing noise, dark noise and read-out noise. Photon signal to noise ratio (S/N) per pixel at count value over 30000 (around 200000e⁻ or 400000 photons) is about 600. After averaging from about 60 spectral channels and at least 5 sets of runs, the S/N becomes greater than 1000; therefore the photon noise is almost negligible. Noise caused by the seeing (scintillation) can be a problem. Namely, due to the "pinhole" imaging, the telescope (spectrograph) effective aperture is very small (around 1.2 mm). But the seeing noise is also suppressed by averaging the signal from 60 spectral channels and the five runs for each observed spectrum. The declared readout noise of the used CCD camera is 25 e⁻ per read operation at -20 °C, which gives S/N over 1000. But, due to problems with water vapor condensation on the camera entrance windows, our working temperature was fixed at -5 °C, and that increased the readout noise. Declared dark current is 13 e⁻/(pixel s) at -20 °C or about 30 e⁻/(pixel s) at our working temperature. Therefore the dark noise, at the exposure times we used, has no significant influence on the errors of measurements. The effect of averaging the signals

from 60 spectral channels and from 5 or more sets of runs on S/N ratio was derived from statistics of measured continuum signal variation. The final S/N is about 400, which is about half of what we expected from a priori estimations. The degradation of S/N is probably due to the nonuniform pixel responsivity across the CCD array. Fortunately, even this S/N allows acceptably accurate brightness measurements.

Since the infrared spectrum is not visible with the naked eye, the appropriate spectral regions have been found using the overlapping of the fourth spectral order in green spectral region with the third spectral order in infrared. The OG2 filter was used as the spectral order separator, which cuts out the green light of the fourth spectral order during the exposure time. The wavelengths in fourth order green spectral region that correspond to wavelengths of the selected telluric lines in third order are listed in fourth and fifth columns of Table 1.

The observations were performed in July and August 2006. During this period 20 observational sets were made. Every spectral region in a set was observed at least five times with exposure times between 0.5 to 1.2 sec, depending on Earth's atmosphere transparency.

The CCD images have been reduced in a simplified manner using IRAF package. No bias or flat-fielding corrections were applied. The dark-frame corrections were performed automatically by CCD camera software for the first several observations, and later the dark frames were taken separately, usually in the beginning, in the middle and in the end of observation, and then subtracted from the images. In several observational sets it was also necessary to rotate the images prior to spectrum extraction, so as to make the spectrograms parallel to the rows of CCD chip. The five frames of each spectral region were averaged into one spectrogram. Background radiation was eliminated from each combined image by subtracting the average signal in pixels not covered by the spectrum.

Each spectrogram has approximately 60 spatially separated spectral channels (60 columns of CCD chip), and the final one-dimensional spectrum is the average value of signal from corresponding columns. The normalization of intensity was done by dividing the measured intensities with a low order polynomial function that was obtained from fitting the observed continuum. Finally, the wavelength calibration was done using the tabulated values (published by Moore et al. 1966) of telluric spectral line pairs in each spectrum.

3. RESULTS AND DISCUSSION

From the observed spectra the equivalent widths of appropriate spectral lines were measured using the SPE software. The equivalent widths of both components ($EW1$ and $EW2$) were measured separately to avoid the influence of other spectral lines that may appear between the components. For further analysis, we used the sum of two components

($EW=EW1+EW2$), because a single rotational quantum number describes both components of the pair. The measured equivalent widths were reduced to the corresponding value at the zenith by taking into account the relative air mass at the moment of observation. Since the observations were made at small zenith distances (z), a simplified formula (sec z) was used for calculation of the relative air mass.

We examined plots of $\ln(EW_J/2J+1)$ against $J(J+1)$ for every observed set (corresponding to each day of observation). Fig. 3 shows a typical example of these plots. The agreement between theory and observation is rather good, but, clearly, it could be made better by discarding the lines with large deviations from the linear fit.

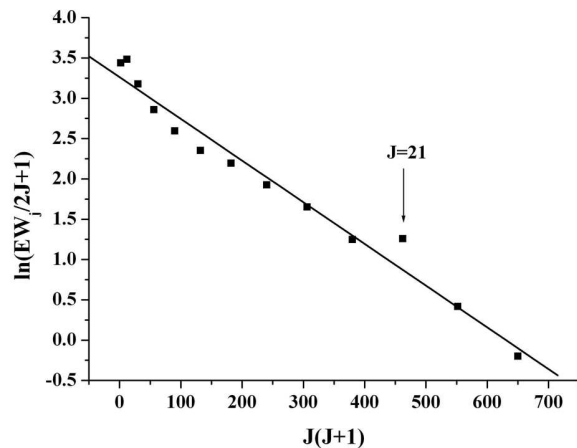


Fig. 3. $\ln(EW_J/2J+1)$ versus $J(J+1)$. Dots represent the observed values and the line is the best linear fit.

As we can see from Fig. 3, the spectral line with rotational quantum number $J=21$ shows the largest discrepancy between observation and theory. The deviation is very similar in every observational set, so it has to be a systematic error. The measured equivalent width of this spectral line is too large. Separate plots for each component of the doublet show the same discrepancy, and the difference is larger for the blue component. Therefore, as it was already mentioned, another blending contributor has to be present in this line. We examined the spectral features in the vicinity of the profile of this line (see Fig. 4) and concluded that the measured higher equivalent width of the blue component¹ is probably due to a small, unidentified line (at 692.305 nm) in its far blue wing and to the blends of water vapor and oxygen molecular lines (formed from nuclei of minor oxygen isotope) situated under its profile. The major disturber of the red component is a relatively strong water vapor line in its red wing. Besides, this range of spectrum is crowded with spectral features that make the determination of continuum level imprecise.

¹In table of solar spectrum wavelengths by Moore et al. (1966) this component was not identified!

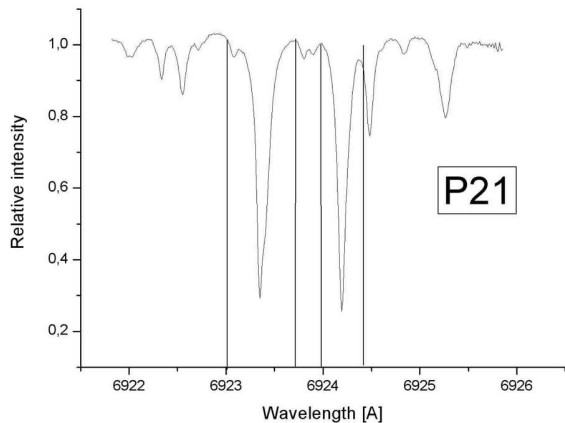


Fig. 4. The observed spectrum with two components of spectral line with $J=21$.

Table 2. Results of fitting statistics of the observed equivalent widths against rotational quantum numbers.

Date	C_5	Error	R	STD
050706	-0,00535	1,59E-04	0,99646	0,03888
280606	-0,00525	1,51E-04	0,99671	0,03679
220706	-0,00501	1,20E-04	0,99773	0,02915
110706	-0,00488	1,25E-04	0,9974	0,0304
200706	-0,0048	6,14E-05	0,99935	0,01498
140706	-0,00475	1,17E-04	0,9976	0,02841
270706	-0,00465	1,57E-04	0,99546	0,03831
250706	-0,00464	8,65E-05	0,99861	0,02109
180706	-0,00463	3,33E-05	0,99979	0,00813
120706	-0,00462	1,30E-04	0,99683	0,0318
260706	-0,00459	1,57E-04	0,99535	0,03825
280706	-0,00458	7,27E-05	0,99899	0,01774
100706	-0,00455	1,44E-04	0,99603	0,03502
70706	-0,00454	1,34E-04	0,99652	0,03274
210706	-0,0045	1,48E-04	0,99567	0,03618
190706	-0,00447	8,31E-05	0,99862	0,02027

In the next step of analysis we discarded this line and repeated the linear fit. We continued discarding lines that didn't agree well with the linear fit until the regression coefficient became greater than 0.995. Following this criterion, the best fit was achieved using spectral lines with $J=9, 11, 13, 15, 17$ and 19 . The errors of determination of C_5 , the standard deviations (STD), and the correlation coefficients (R) for these six lines were obtained from the fits statistics, and are listed in Table II. We left out four incomplete observation sets (not completed because of technical problems and clouds during observations) from Table II, which thus shows the results for 16 observational sets. The regression coefficients for all observational sets are greater than 0.995, indicating an excellent agreement between theoretical predictions and observation. Fig. 5 shows an ex-

ample of the plot of the observed equivalent widths against rotational quantum numbers with the best linear fit, after all the deviant lines have been discarded. As one can see, the agreement between observation and theory is perfect.

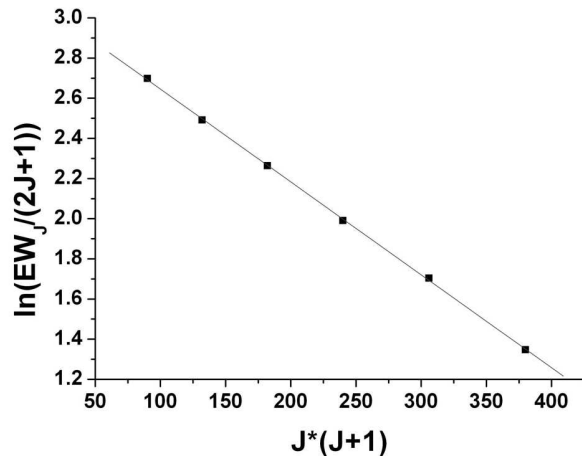


Fig. 5. Observed equivalent widths against rotational quantum numbers (dots) and the best linear fit (line) for $J = 9, 11, 13, 15, 17, 19$.

4. CONCLUSIONS

At Belgrade Astronomical Observatory a new observational program for monitoring telluric lines is being established. Thirteen infrared molecular oxygen lines with odd rotational quantum numbers from 1 to 25 of P branch from B atmospheric band were selected for observation. The suitability of these spectral lines for the program was investigated by comparing the relation between observed equivalent widths and rotational quantum numbers with theoretical prediction. For six spectral lines with rotational quantum numbers from 9 to 19, an excellent agreement between observation and theory was found. Therefore, we conclude that these six lines are the most suitable for our observational program. The agreement between theory and observation for the rest of the lines was also acceptable, but for the inclusion of these lines into the program it would be necessary to further investigate the causes of the discrepancy between observations and theory.

To improve the quality of our observations we plan to replace the old SBIG ST6 CCD camera with a new Apogee Alta U47+ CCD camera, which is more sensitive in infrared spectral region and has an array size of 1024x1024 pixels with pixel size of $13 \times 13 \mu\text{m}$. Its larger chip (about 13 mm long) will enable to cover at least two pairs of rotation line doublets, and its smaller pixel size will allow better sampling resolution. We also plan to rearrange the spectrograph to deliver the sunlight to it by projecting the solar image onto the entrance slit. This will improve the grating illumination and, consequently, the spectral resolution.

Acknowledgements – The work is a part of the project "Stellar and Solar Physics" (No. 146003) supported by the Ministry of Science and Environment Protection, Republic of Serbia. One of the authors (OL) acknowledges scholarship of the Ministry of Science and Environment Protection of Republic of Serbia (No. 451-03-0358/2006-02).

REFERENCES

- Beckers, J.M., Bridges, Ch.A., Gilliam, L.B.: 1976, A High Resolution Spectral Atlas of the Solar Irradiance From 380 to 700 Nanometers, Volume II: Graphical Form, Sacramento Peak Observatory.
- Guineva, V., Werner, R.: 2006, The international Journal of Research and Applications (published by Balkan, Black Sea and Caspian Sea Regional network on Space Weather Studies), v.1, N1, pp. 56-59.
- Kubicela, A.: 1975, *Publ. Astron. Obs. Beograd*, **20**, 47.
- Moore, Ch.E., Minnaert, M.G.J., Houtgast, J.: 1966, The Solar Spectrum from 2935 Å to 8770 Å, National Bureau of Standards Monographs 61, Washington, D. C.
- Schadee, A.: 1964, *B.A.N.*, 17, No 5, 311-357.
- Schadee, A.: 1966, IAU Symposium 26 (Ed. H. Hubenet), Academic Press, London, p. 92.
- Vince, I., Kubicela, A. and Arsenijević, J.: 1988, *Bull. Obs. Astron. Belgrade*, **139**, 25.

БЕОГРАДСКИ ПРОГРАМ ПОСМАТРАЊА ТЕЛУРСКИХ ЛИНИЈА

I. Vince¹, P. Kos², O. Latković¹, N. Martinović³, M. Gošić³ and J. Stojadinović³

¹*Astronomical Observatory, Volgina 7, 11160 Belgrade 74, Serbia*

²*University Paris 7 - Denis Diderot, France*

³*Department of Astronomy, Faculty of Mathematics, Studentski trg 16, 11000 Belgrade, Serbia*

UDK 520.84

Стручни рад

Нови посматрачки програм за праћење телурских линија је успостављен на Астрономској опсерваторији у Београду. Крајњи циљ овог програма је добијање информација о особинама Земљине атмосфере моделирањем посматраних профила телурских линија. Програм се састоји од посматрања инфрацрвених линија молекулног кисеоника, које

су одабране према осетљивости наше CCD камере. У овом раду описани су критеријуми за одабир спектралних линија за програм, опрема и поступци коришћени током посматрања и редукције, преглед прелиминарних резултата са проценом прецизности посматрања, и кратка дискусија о слагању теорије са нашим мерењима.